Pharmaceutical Sciences Asia

Pharm Sci Asia 2026; 53(1), 78-91

DOI:10.29090/psa.2026.01.25.4856

Research Article

Formulation and *in vitro* cytotoxicity evaluation of andrographolide-loaded nano delivery systems in the Renca renal cancer cell line

Nhat-Trang Nguyen[1], Ngoc-Quang Do[3], Tran-Mai-Phuong Nguyen[1], Cong-Khanh Cao[2], Thi-Thu-Hien Duong[3], Nguyen-Thach Tung[1*]

[1] Hanoi University of Pharmacy, Hanoi, Vietnam
[2] National Institute for Food Control, Hanoi, Vietnam
[3] The University of Sydney, Sydney, Australia

ABSTRACT

Andrographolide (ADG), which exhibits a variety of pharmacological effects, poses significant formulation challenges due to its limited solubility. This study aimed to enhance ADG's solubility through two drug delivery systems: polymeric micelles and self-nanoemulsifying drug delivery systems (SNEDDS). The ADG-loaded polymeric micelles were prepared by synthesizing POEGMA-*b*-PVBA via RAFT polymerization, followed by ADG conjugation in methanol. The structure and molecular weight of POEGMA and POEGMA-*b*-PVBA were confirmed by ^{1}H-NMR spectroscopy. ADG-loaded SNEDDS were prepared by screening components and constructing ternary phase diagrams, followed by droplet size analysis to determine the optimal formulations. Both systems were evaluated for cytotoxicity against the Renca cell line. The synthesized polymer was POEGMA58-*b*-PVBA12 and then conjugated with ADG to form micelles, exhibiting a nanoparticle size of 115.0 ± 0.7 nm. ADG was also prepared as SNEDDS with Labrafil 1944 CS, Tween 80, and Transcutol HP, with a particle size of 145.5 ± 2.7 nm. Cytotoxicity results showed that the cell viability reduced significantly to 74.2% after being exposed to ADG-loaded SNEDDS at 200 µM, while ADG polymeric micelle and suspension showed no differences. The results suggested that SNEDDS was more effective than polymeric micelles in enhancing the cytotoxicity of ADG against the Renca cell line.

Keywords:
Andrographolide; SNEDDS; Polymeric micelles; Renal cell carcinoma; Kidney cancer

1. INTRODUCTION

Data from WHO Cancer Today shows that in 2022, kidney cancer was the 14th most common cancer, with the mortality rate ranked 16th in the world. There were around 434,000 cases and 155,000 deaths worldwide, with the number of incidents significantly higher in Asia, Europe, and North America. Remarkably, renal cell carcinoma (RCC) accounts for the majority of kidney tumors. Kidney cancer is usually diagnosed at a stage amenable to surgical intervention, and improving patient's conditions. However, metachronous distant metastases still develop in about one-third of patients who have received surgery for limited or regional extension kidney tumors[1], significantly affecting the chances of survival for patients. Even though other treatments, such as chemotherapy and drug therapy, are the most common approaches, they still pose significant challenges. Amid the search for effective treatment methods, natural compounds have attracted increasing attention due to their potential therapeutic benefits. Andrographolide (ADG) is a natural diterpenoid isolated from the stems and leaves of *Andrographis paniculata*. In various studies, andrographolide exhibited pharmacological effects such as

***Corresponding author:**
* Nguyen-Thach Tung Email: nguyenthachtung@hup.edu.vn

anti-inflammatory, anti-oxidant, and anti-bacterial[2–4]. ADG also has the potential to treat other illnesses such as Parkinson's[5] and especially exhibits anticancer activities. Previous studies have shown that ADG is a promising drug for colon cancer by suppressing TLR4/NF-κB/MMP-9 signaling pathway[6], and for lung cancer by reducing levels of VEGF and TGF-β1[7], indicating that ADG is a potential substance for cancer treatment. However, while ADG has been investigated in combination therapy in renal carcinoma cells, no studies have focused on the pharmaceutical development of ADG to overcome its limitations in the treatment of kidney cancer. Therefore, this study concentrates on developing pharmaceutical strategies to enhance ADG and evaluate their therapeutic effect on this type of cancer.

Despite various therapeutic functions, a major limitation of ADG is its low aqueous solubility (3.29 ± 0.73 µg/mL at 25°C), leading to low oral bioavailability. To overcome this problem, identifying and choosing a suitable drug delivery system is significantly important. Over the past few decades, nanotechnology, which is a rapidly growing area, has offered a host of new opportunities in medicine and healthcare, including the ability to deliver poorly water-soluble drugs[8]. Nanoparticles can also cross biological membranes such as the blood-brain barrier and target cancer by accumulating and entrapping in tumors[9]. Among various approaches, nanopolymer and lipid-based systems have been shown to improve solubility and bioavailability because of their small particle size and the ability to encapsulate hydrophobic drugs[10].

Lipid-based drug delivery systems, particularly self-nanoemulsifying drug delivery systems (SNEDDS), are known to improve the solubility and bioavailability of poorly water-soluble drugs[11]. Consisting of oils, surfactants, co-surfactants, and drug substances, these mixtures, when agitated gently with aqueous phase, such as GI fluids, will form nanoemulsions spontaneously with particle sizes of 100-250nm[12]. These nanoemulsion droplets contain dissolved drugs, providing a large interfacial area for absorption and facilitating it to cross the biological membrane[13]. In earlier literature, many have demonstrated great improvement for lipophilic compounds such as chlorpromazine and orlistat in drug solubility and bioavailability when using the SNEDDS system[14,15].

Moreover, polymeric drug delivery systems have attracted attention owing to their ability to control release and deliver stimuli-responsive systems that could target a specific site, thus enhancing therapeutic benefits and minimizing side effects[16]. In this context, polymeric micelles have emerged as a nanocarrier system, outstanding for targeted delivery of hydrophobic drugs. With the core-shell structures, drugs are encapsulated in the hydrophobic core while still being stabilized with an external aqueous environment, thus enhancing solubility and stability for drug substances[17]. To further enhance the stability and functionality of polymeric micelles, reversible addition-fragmentation chain transfer (RAFT) polymerization has been applied in this study. RAFT polymerization is a reversible deactivation radical polymerization, with unique characteristics like construction for complex macromolecular architectures, the ability to perform in aqueous media, and better control over molecular weight[18,19].

Therefore, this study aims to prepare and characterize ADG-loaded polymeric micelles by using RAFT polymerization and ADG-loaded SNEDDS to enhance drug solubility and absorption. We also compared anticancer activities of these systems on the Renca cell line – a mouse renal cell carcinoma (RCC) cell line with that of ADG suspension.

2. MATERIALS AND METHODS

2.1 Materials

ADG was supplied by AKScientific (India). Alamar Blue, Trypan Blue, and RPMI 1640 medium were supplied by Sigma-Aldrich (USA); Labrafac PG, Labrafac lipophile WL 1349, Labrafil M 1944 CS, Labrasol, Maisine CC, Transcutol HP, and Capryol 90 were obtained from Gattefossé (France); Tween 80 was obtained from Singapore.

Oligo(ethylene glycol) methyl ether acrylate; 4-cyano-4 (phenylcarbonothioylthio)pentanoic acid; 2,2'-Azobisisobutyronitrile; Vinyl benzylaldehyde were obtained from Sigma-Aldrich (USA). Mineral oil was supplied by ChemSupply – Australia.

2.2. Preparation of ADG-loaded micelle polymer

2.2.1. Synthesis of POEGMA macro-RAFT agent

The macro-RAFT agent was prepared according to a published procedure[20]. Monomer oligo(ethylene glycol) methyl ether acrylate (OEGMA) (5.00 g; 1.67 $x10^{-3}$ mol), RAFT agent 4-cyano-4-(phenylcarbonothioylthio)pentanoic acid (CPADB) (7.76 x 10^{-2} g; 2.78 x 10^{-5} mol) and 2,2'-Azobisisobutyronitrile (AIBN) (4.6 x 10^{-3} g; 2.78 x 10^{-5} mol) was dissolved in 20 mL of toluene within a vial under magnetic stirring. The vial was then sealed with a rubber septum and purged with nitrogen gas for 30 minutes to remove oxygen completely. Next, the reaction mixture was heated at 70°C. After 17 hours, the polymerization was terminated by cooling the sample in an ice bath for 5 minutes. The POEGMA polymer was purified three times by precipitation with mineral oil (boiling in the range of 40-60°C), followed by centrifugation (7000 rpm in 15 minutes) (Eppendorf,

England, model 5430R) and then dried in a vacuum oven (Daihan, Korea) at room temperature. The samples were stored at 4°C until being used for further chain extension. The conversion (%) of monomers during the polymerization was determined by ^{1}H-NMR, with the vinyl proton peaks (6.1 and 5.6 ppm) and the ester proton peak (4.1 ppm). The conversion (%) of monomers was calculated using the following equation:

$$\alpha^{OEGMA} = \frac{\int 4.1\ \text{ppm(17h)}}{\int 4.1\ \text{ppm(17h)} + 2\int 5.6\ \text{ppm(17h)}} \times 100\%$$

The molecular weight of the POEGMA macro-RAFT agent was calculated from ^{1}H-NMR as follows:

$$M_{n,POEGMA} = \alpha^{OEGMA} \times \frac{[OEGMA]}{[CPADB]} \times M_{W,OEGMA} + M_{W,CPADB}$$

In which [OEGMA], $M_{W,\ OEGMA}$ and [CPADB], $M_{W,\ CPADB}$ represent the amount of substance (in moles) and molecular weight of the OEGMA monomer and the RAFT agent in the reaction, respectively.

2.2.2. Synthesis of POEGMA-b-PVBA

POEGMA consisting of 58 repeat units ($M_{n,\ NMR}$ = 17502 g/mol) was used as a macro-RAFT agent for chain extension with vinyl benzylaldehyde (VBA). The number of repeated units of POEGMA was determined using ^{1}H-NMR to analyze the monomer conversion rate. The macro-RAFT agent POEGMA (1.00 g; 1.14 x 10^{-4} mol) and VBA (0.3020 g; 2.29 x 10^{-3} mol) were dissolved in 5 mL of acetonitrile and sealed with a rubber septum. To ensure an oxygen-free environment, the reaction mixture was purged with nitrogen gas for 30 minutes in an ice bath. The polymerization proceeded in a 70°C oil bath overnight and was terminated by cooling the reaction mixture in ice for 5 minutes. Purification of the polymer involved repeated precipitation (three times) in excess diethyl ether, then centrifugation (7000 rpm for 15 minutes). After that, the polymer was dried under reduced pressure at room temperature. The conversion (%) of VBA was calculated from the ^{1}H-NMR of the reaction mixture using the following equation:

$$\alpha^{VBA} = \frac{\int 9.8\ \text{ppm(17h)}}{\int 9.8\ \text{ppm(17h)} + \int 10\ \text{ppm(17h)}} \times 100\%$$

The peaks at 9.8 ppm and 10 ppm correspond to the aldehyde proton of PVBA polymer and VBA monomer, respectively.

The molecular weight of POEGMA-*b*-PVBA polymer was calculated by ^{1}H-NMR spectrum using this formula:

$$M_{n,POEGMA-b-PVBA} = \alpha^{VBA} \frac{[VBA]}{[POEGMA]} \times M_{W,VBA} + M_{n,POEGMA}$$

[POEGMA], $M_{W,\ POEGMA}$ and [VBA], $M_{W,\ VBA}$ represent the amount of substance (in moles) and the molecular weight of the macro-RAFT POEGMA agent and the VBA monomer in the reaction, respectively.

2.2.3. Determination of critical micelle concentration

The critical micelle concentration of POEGMA58-*b*-$PVBA_{12}$ was determined using the conductivity method. A stock solution of the polymer (10 µM) was prepared in deionized water and incrementally added to 50 mL of deionized water, giving polymer concentrations ranging from 0.20 µM to 3.59 µM. The conductivity of each solution was measured, and the obtained values were plotted as conductivity versus polymer concentration.

2.2.4. Conjugation of POEGMA-b-PVBA to ADG

POEGMA-*b*-PVBA polymer and ADG were dissolved in methanol. Next, ADG was added gradually to the polymer and stirred gently for 10 minutes. This mixture was then added dropwise to the aqueous phase (distilled water) while maintaining a slow stirring speed overnight to ensure that the methanol evaporated completely to obtain the polymeric micelle system. This system is stored at room temperature until required for further analysis.

2.3. Preparation of ADG-loaded SNEDDS

2.3.1. Solubility study

ADG's solubility in different oils, surfactants, and co-surfactants was conducted by adding excess ADG to 5g of each vehicle in a centrifugal tube. Then the mixtures were kept in a shaking water bath at 125 rpm, 37°C for 72 hours to reach equilibrium, followed by centrifugation (Eppendorf, England, model 5430R) at 6000 rpm for 10 minutes. The supernatant was filtered through a membrane filter (0.45 µm) and diluted properly with methanol before being measured by HPLC to analyze andrographolide concentration.

HPLC system (Shimadzu, Japan) consisted of UV detection with a C18 column (5 µm, 250 x 4.6 mm). The mobile phase was composed of methanol-water (55:45) at a flow rate of 1.0 mL/min, the injection volume was 20 µl. The detection wavelength was set at 225 nm to determine the concentration of ADG[21].

2.3.2. Construction of ternary phase diagrams

To identify the range of nanoemulsion existence, pseudo-ternary diagrams were constructed using the H_2O

citation method. The weight ratio of surfactant to co-surfactant (S_{mix}) varied as 1:0, 1:2, 1:1, 2:1, 3:1, and 4:1. At each S_{mix} ratio, the oil to S_{mix} weight ratio varied from 1:9, 2:8, 3:7, 4:6, 5:5, 6:4, 7:3, 8:2, 9:1. Then, distilled water was added dropwise to the oily mixture while gently shaking it. After being equilibrated, the mixtures were assessed visually. The system will transition from a clear to a turbid state, corresponding to different physicochemical structures: microemulsion, nanoemulsion, and coarse emulsion. Based on these diagrams, the optimized concentration of oil and S_{mix} was selected for further studies.

2.3.3. Preparation and characterization of ADG-loaded SNEDDS

ADG was dissolved in the combination of the chosen oil, surfactant, and co-surfactant at different ratios, followed by the addition of a specific quantity of water to the mixture while stirring. The resulting mixture gave SNEDDS. Formulations with varying ratios of the components were prepared and the droplet size was determined by Zetasizer Nano ZS90 (Malvern, England) to find the optimal ratio.

2.4. Preparation of ADG suspension

ADG suspension was prepared by dispersing the drug substance in distilled water at different desired concentrations equivalent to 1, 5, 10, 50, 100, and 200 μM of ADG. The prepared suspensions were then subjected to subsequent experiments.

2.5. Cell culture

The Renca cell line was grown and maintained in T-25 cell culture flasks with a vent cap (Greiner Bio-one, Austria) containing RPMI 1640 medium with 10% fetal bovine serum. Cell incubation was performed at 37°C, under a humidified atmosphere containing 5% CO_2, and cells were allowed to grow to approximately 80% confluence. Cells were detached by 0.05% trypsin in the PBS buffer, then stained with trypan blue, and loaded onto a hemocytometer to determine cell density. All experiments were performed six times.

2.6. Cytotoxicity assays

The Renca cell lines were seeded into 96-well plates at a density of 10^4 cells/well and incubated in 5% CO_2 at 37°C. After 24 hours, the culture medium was replaced by different concentrations of ADG-loaded micelle polymer, SNEDDS, and suspension, as well as the blank samples. After 72 hours of incubation, the medium was removed, and the growth of cells was determined by Alamar Blue. Alamar Blue was filtered through a 0.45 μm filter and then diluted with RPMI 1640 medium at a 2:8 ratio. Each well was added 100 μL of Alamar Blue and incubated for 6 hours. The cell staining procedure was carried out under light-protected conditions, as Alamar blue is light-sensitive. Finally, absorbance was read at 550 nm using a Victor X plate reader (Perkin Elmer, USA) and Perkin Elmer Analysis software. All experiments were conducted six times. The dose-response curves were expressed as percentages relative to the control sample (containing only the growth medium) and the IC_{50} inhibitory concentration was estimated by regression analysis.

2.7. Statistical analysis

All experiments were repeated at least 3 times, data were expressed as the mean value ± SD. Unpaired Student's *t*-tests were performed to compare differences between the two formulations, while one-way analysis of variance (ANOVA) was used to evaluate differences in various formulations. The data was considered statistically significant at $p < 0.05$.

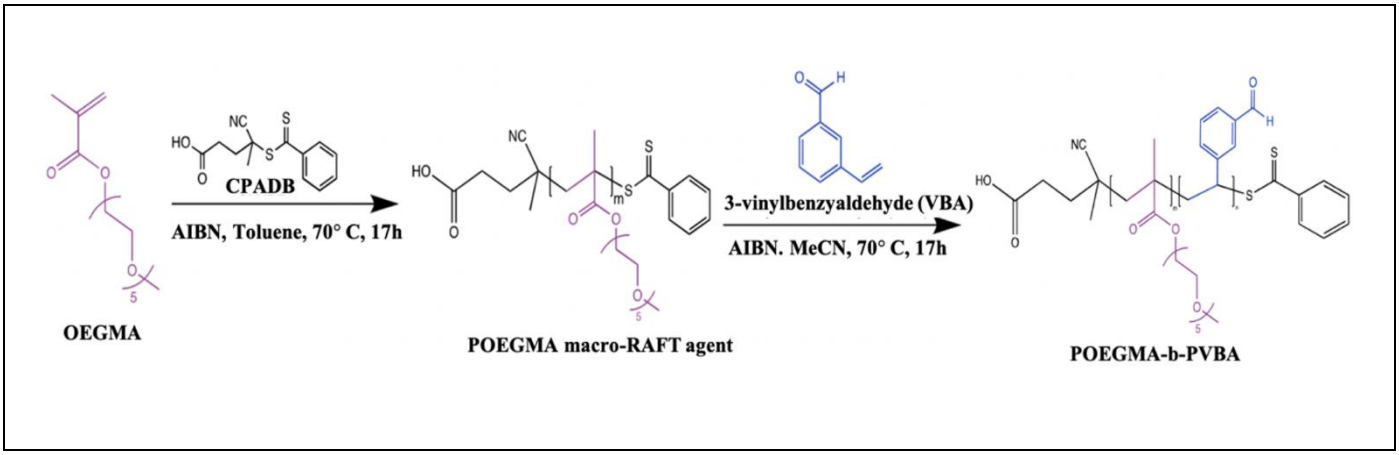

Figure 1. Schematic representation for the preparation of POEGMA-*b*-PVBA polymer by RAFT polymerization

3. RESULTS

3.1. Formulation of ADG-loaded micelle polymer

3.1.1. Synthesis of POEGMA-b-PVBA polymer

POEGMA-*b*-PVBA polymer was synthesized by the reversible chain transfer polymerization (RAFT) technique (Figure 1).

Poly((oligoethylene glycol) methyl ether methacrylate) (POEGMA) macro-RAFT agent, synthesized in toluene at 70°C in the presence of 4-cyano-4-(phenylcarbonothioylthio)pentanoic acid (CPADB), acted as a RAFT agent and oligo(ethylene glycol) methacrylate (OEGMA) as monomer. The conversion (%) of the monomer (α^{OEGMA} = 95.8%) and the molecular weight of the macro-RAFT agent ($M_{n,POEGMA}$ = 17502 g/mol) were determined by ^{1}H-NMR (Figure 2) by comparing the vinyl proton signals (at 6.1 and 5.6 ppm) with ester -OCH_2 proton signals (at 4.1 ppm). The polymer product underwent purification through three times of precipitations in petroleum solvent.

Next, POEGMA was chain extended with 3-vinylbenzylaldehyde (VBA) to form the POEGMA-*b*-PVBA block copolymer. The attachment of VBA was confirmed by ^{1}H-NMR using signals at 9.8 ppm and 10 ppm, attributed to the aldehyde group of the polymer and monomer of VBA, respectively (Figure 3). The conversion rate (%) of VBA was determined to be about 54%. The molecular mass of the block copolymer $M_{n,POEGMA\text{-}b\text{-}PVBA}$ was calculated to be 18886 g/mol.

The resulting polymer is $POEGMA_x$-*b*-VBA_y, with x and y being 58 and 12, respectively. POEGMA-*b*-PVBA block copolymer consists of a longer hydrophilic block of 58 OEGMA units and a shorter hydrophobic block of 12 VBA units. If a longer block of VBA were used, the polymer would be less soluble in water.

To further evaluate the self-assembly behavior of this polymer in aqueous solution, the critical micelle concentration (CMC) of POEGMA-*b*-PVBA was determined by the conductivity method. At low concentrations, the conductivity increased linearly with polymer concentration due to the presence of free ionic groups. Once micelle is formed, part of these ionic groups become shielded inside the micelles,

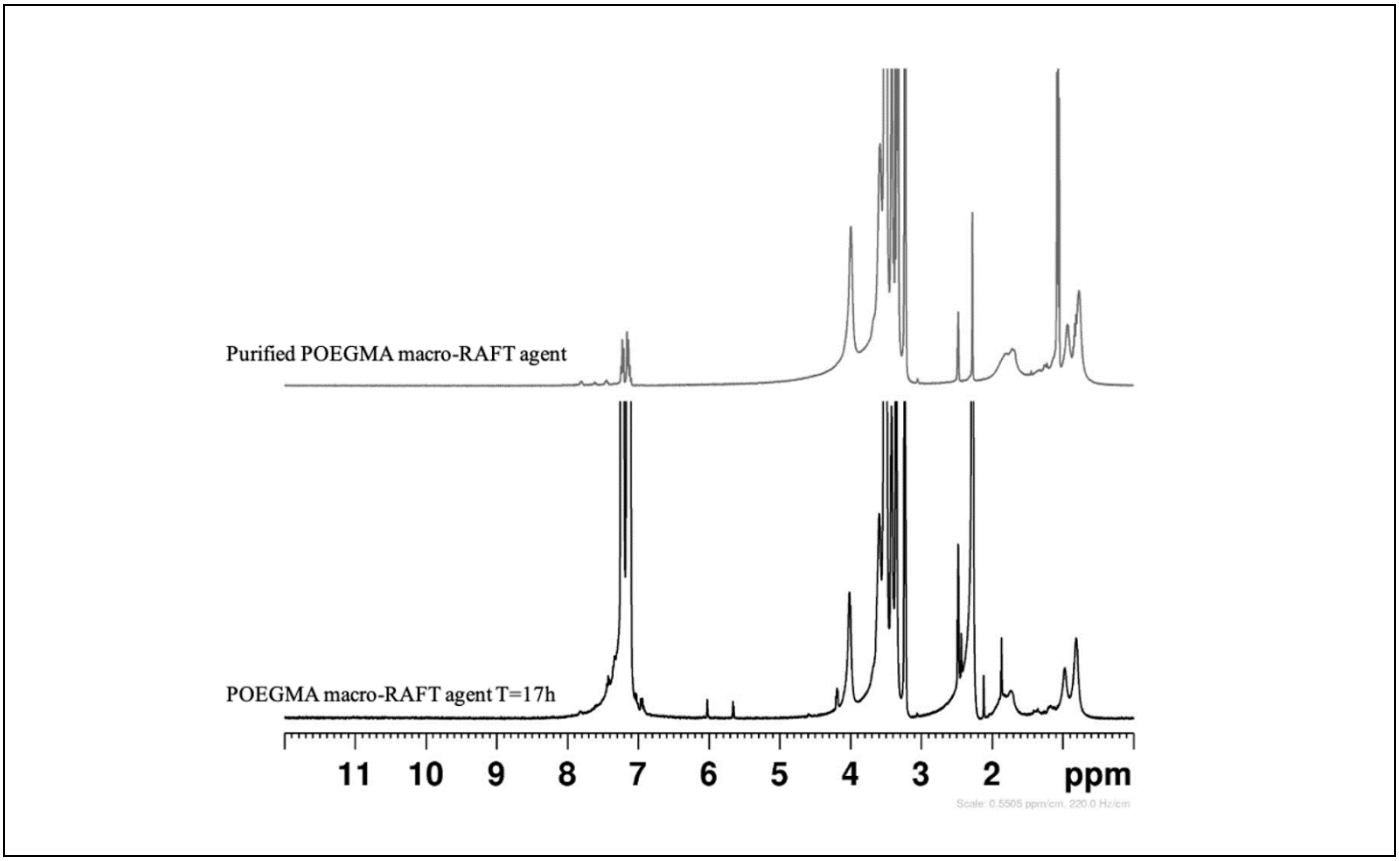

Figure 2. ^{1}H NMR spectra of POEGMA macro-RAFT agent

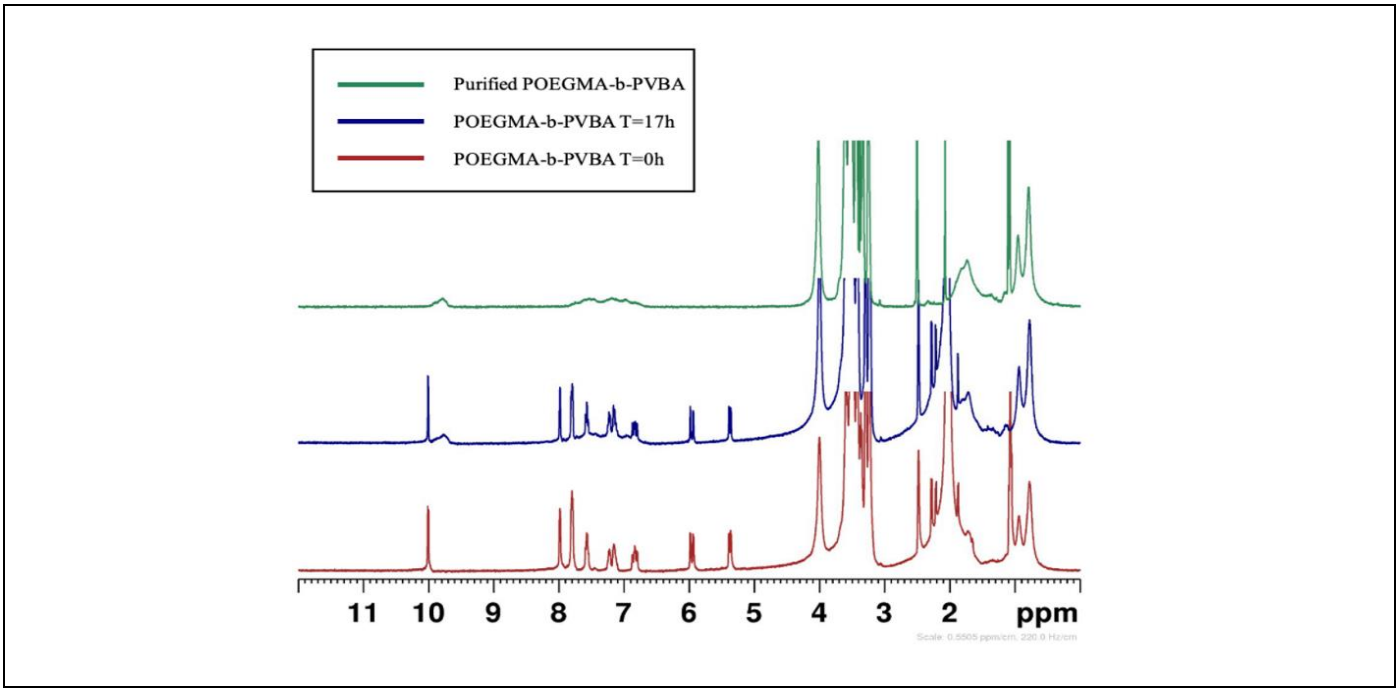

Figure 3. ^{1}H NMR spectra of POEGMA-*b*-PVBA polymer

leading to the change in the slope of the conductivity curve. The intersection of the two linear regions was taken as the CMC, which was determined to be 0.26 × 10^{-5} M (47.2 mg/L) (Figure 4). This low CMC value exhibits an ability to form micelles at a low concentration, potentially enhancing bioavailability by avoiding the disintegration of micelle structures under diluted conditions within the body[22,23].

The hydrophobic micelle core (PVBA) interacts and encapsulates ADG - a poorly water-soluble substance. The compatibility between the micelle core and ADG is explained by the Van der Waals bonds between the benzene ring (PVBA) and the cyclodecane ring system in ADG, along with hydrogen bonding between the hydroxyl group (H) and the aldehyde group (O).

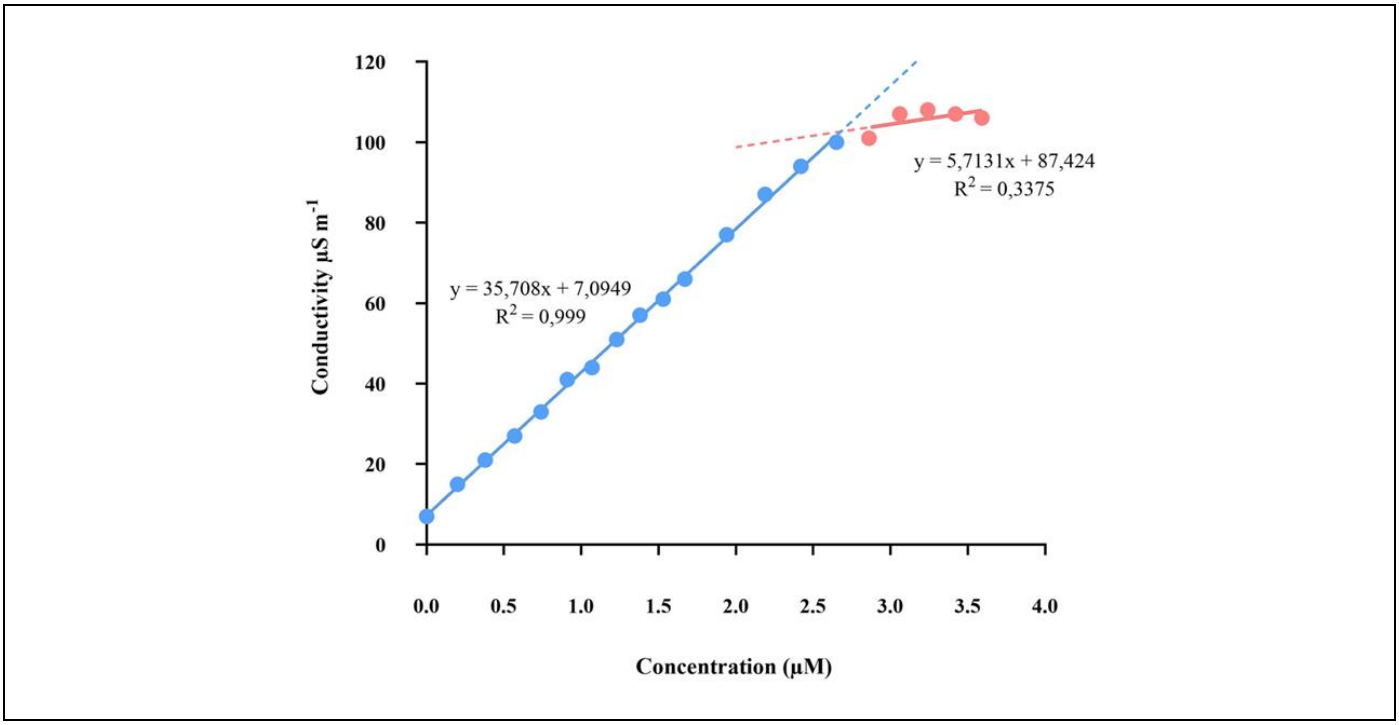

Figure 4. Conductivity versus concentration plot of POEGMA-*b*-PVBA solutions for CMC determination. The breakpoint indicates the CMC at 0.26 × 10^{-5}M.

Table 1. Compositions and characterization of various ADG polymeric micelle formulations (mean ± SD, n=3).

	ADG (mg)	Polymer (mg)	Water (mL)	Size (nm)	PDI
P1	0.25	10	1.00	58.4 ± 2.9	0.480 ± 0.045
P2	0.25	20	1.00	43.3 ± 0.1	0.557 ± 0.003
P3	0.25	30	1.00	25.4 ± 1.0	0.390 ± 0.014
P4	0.50	30	1.00	167.0 ± 18.1	0.375 ± 0.038
P5	0.50	40	1.00	144.6 ± 24.8	0.255 ± 0.039
P6	0.50	50	1.00	115.0 ± 0.7	0.172 ± 0.008
P7	1.00	60	1.00	800.1 ± 208.8	0.729 ± 0.124
P8	1.00	70	1.00	753.5 ± 104.3	0.863 ± 0.093
P9	1.00	80	1.00	627.4 ± 161.28	0.928 ± 0.103

3.1.2. Preparation and characterization of ADG-loaded micelle polymer

Polymer micelle samples containing different concentrations of ADG and polymer were prepared, and the particle size was evaluated by dynamic light scattering (Table 1).

The average particle size of ADG suspension and POEGMA-*b*-PVBA polymer was also determined (Table 2). The results demonstrated a trend of increasing particle size with higher drug concentration. With the same amount of ADG, the particle size decreased with a higher amount of polymer. At the concentration of 0.25 mg/mL ADG, all three formulations showed an average size below 60nm, but a high PDI, which indicated a broad size distribution. As the average particle size of polymeric micelles without ADG was 22 nm, this small size could be attributed to an excess amount of polymer used for drug-loading. At the concentration of 1.00 mg/mL ADG, the particle size of the three formulations ranged from 600-800 nm, which was slightly lower than that of the ADG suspension in water (1005 nm), indicating that the system was overloaded with drug substances.

To maximize drug loading while maintaining nanoparticle size, the formulation P6 was selected for further studies. The narrow particle size distribution of P6 (0.172 ± 0.008) showed that the amount of polymer used was sufficient to encapsulate ADG at the concentration of 0.5 mg/mL, thereby confirming that this was the optimal ADG and polymer ratio.

3.2. Formulation and characterization of SNEDDS

3.2.1. Solubility study

The ADG solubility in a variety of oils, surfactants, and cosurfactants was analyzed to select suitable excipients for the formulations. The results of this study are shown in Table 3.

Among the oils, it was found that ADG exhibited the highest solubility in medium-chain triglyceride Capryol 90 (12.43 ± 0.43 mg/g). However, long-chain triglycerides can improve intestinal lymphatic transport of drugs and prevent first-pass metabolism[24], which is also the cause of ADG's poor oral bioavailability. Thus, Labrafil M 1944 CS, a long-chain triglyceride that has the best ability to dissolve ADG, was chosen as the oily phase.

Tween 80 was able to dissolve 27.27 ± 1.72 mg/g ADG, better than other surfactants such as Labrasol, Tween 20, and Cremophor. Previous studies showed that nonionic surfactants could enhance the permeability and absorption of drugs by inhibiting P-glycoprotein[25]. In addition, nonionic surfactants tend to be less irritating and remain relatively stable to changes in pH and ionic strengths that can occur in the gastrointestinal tract. Meanwhile, co-surfactant Transcutol HP (33.56 ± 0.54 mg/g) showed the highest solubility for ADG. Therefore, Tween 80 and Transcutol HP were selected as the surfactant and co-surfactant for SNEDDS formulation.

Table 2. The particle size of ADG suspension and POEGMA-*b*-PVBA polymer (mean ± SD, n=3).

	Z-average (nm)	PDI
ADG suspension	1000.5 ± 111.5	0.783 ± 0.120
POEGMA-*b*-PVBA polymer	22.0 ± 0.05	0.067 ± 0.007

Table 3. Solubility of Andrographolide in various components (mean ± SD, n=3).

	Components	Solubility of Andrographolide (mg/g)
Oil	Capryol 90	12.43 ± 0.43
	Labrafac PG	4.61 ± 0.65
	Labrafac lipophile WL 1349	1.81 ± 0.24
	Labrafil M 1944 CS	11.99 ± 0.15
	Maisine CC	5.57 ± 0.35
	Labrafil M 2125 CS	4.36 ± 0.26
	IPM	1.53 ± 0.16
Surfactants	Tween 80	27.27 ± 1.72
	Labrasol	25.28 ± 1.00
	Tween 20	24.62 ± 1.97
	Cremophor RH40	23.33 ± 1.18
	Cremophor EL	22.45 ± 0.81
	Span 80	2.58 ± 0.15
Co-surfactants	Transcutol HP	33.56 ± 0.54
	Ethanol	29.82 ± 1.42
	PEG 300	25.01 ± 2.08
	PEG 400	30.77 ± 0.82

3.2.2. Construction of ternary phase diagrams

Ternary diagrams were constructed without ADG to find the nanoemulsification area of the selected systems as well as the suitable concentrations of various components (Figure 5).

It could be observed that the area of nanoemulsion increased gradually with the increasing ratio of surfactant to co-surfactant and exhibited the largest area at a ratio of 4:1. However, when using only surfactants, the region decreased significantly. Similar observations have been reported in the literature that co-surfactants are essential for the formation and extension of emulsion areas[26,27]. Co-surfactants could contribute to reduced interfacial tension significantly and make self-emulsification easier when combined with surfactants. Surfactants and co-surfactants adsorb at the oil-water interface, lowering the interfacial tension and increasing the resistance to droplet coalescence, thereby enhancing the thermodynamic stability of nanoemulsions. Additionally, co-surfactants penetrate the surfactant film, creating spacing between surfactant molecules and improving interfacial flexibility[28]. This suggests that at a certain low proportion, the co-solvent (Transcutol HP) plays a supportive role in enhancing the surfactant's (Tween 80) ability to reduce interfacial tension. At this optimal ratio, the co-solvent helps to fluidize the interfacial film, facilitating the formation of stable nano-sized droplets. However, when the proportion of co-solvent becomes too high, it begins to disrupt the integrity of the interfacial film, weakening its stabilizing effect. As a result, the emulsifying capacity of the system decreases, leading to a narrower nanoemulsion region. Thus, the ratio of surfactant to co-surfactant (S_{mix}) was fixed at 4:1 for further studies.

3.2.3. Characterization

The droplet size of various formulations was measured to identify the appropriate ratio of oil and S_{mix} (Table 4).

Overall, at higher surfactant concentrations, the droplets were relatively smaller, and globule sizes also grew with the increase in the quantity of oil and S_{mix}. Increased concentration of surfactants may result in smaller droplet sizes due to the closely packed surfactant films at the water-oil interface, which stabilize and reduce the surface tension. The size of the globules in a nanoemulsion plays a critical role in determining both the rate and extent of drug dissolution and absorption in the gastrointestinal tract. Small droplet sizes could present great stability by reducing the tendency for gravitational separation and increasing surface area, thereby influencing dissolution rate and bioavailability[29]. Moreover, it could be suggested that a higher proportion of S_{mix} improves emulsification efficiency, resulting in smaller droplet sizes. At O: S_{mix} = 3:7, higher oil content increases droplet size, which could be explained by higher internal phase volume and potential surfactant insufficiency to stabilize all droplets. Systems with a mean droplet size below 200 nm fulfill the criteria of SNEDDS. Among all the formulations, F1 exhibited the smallest droplet size (92.6 ± 1.3 nm), but the highest droplet size distribution (0.544 ± 0.000), indicating a high size distribution and

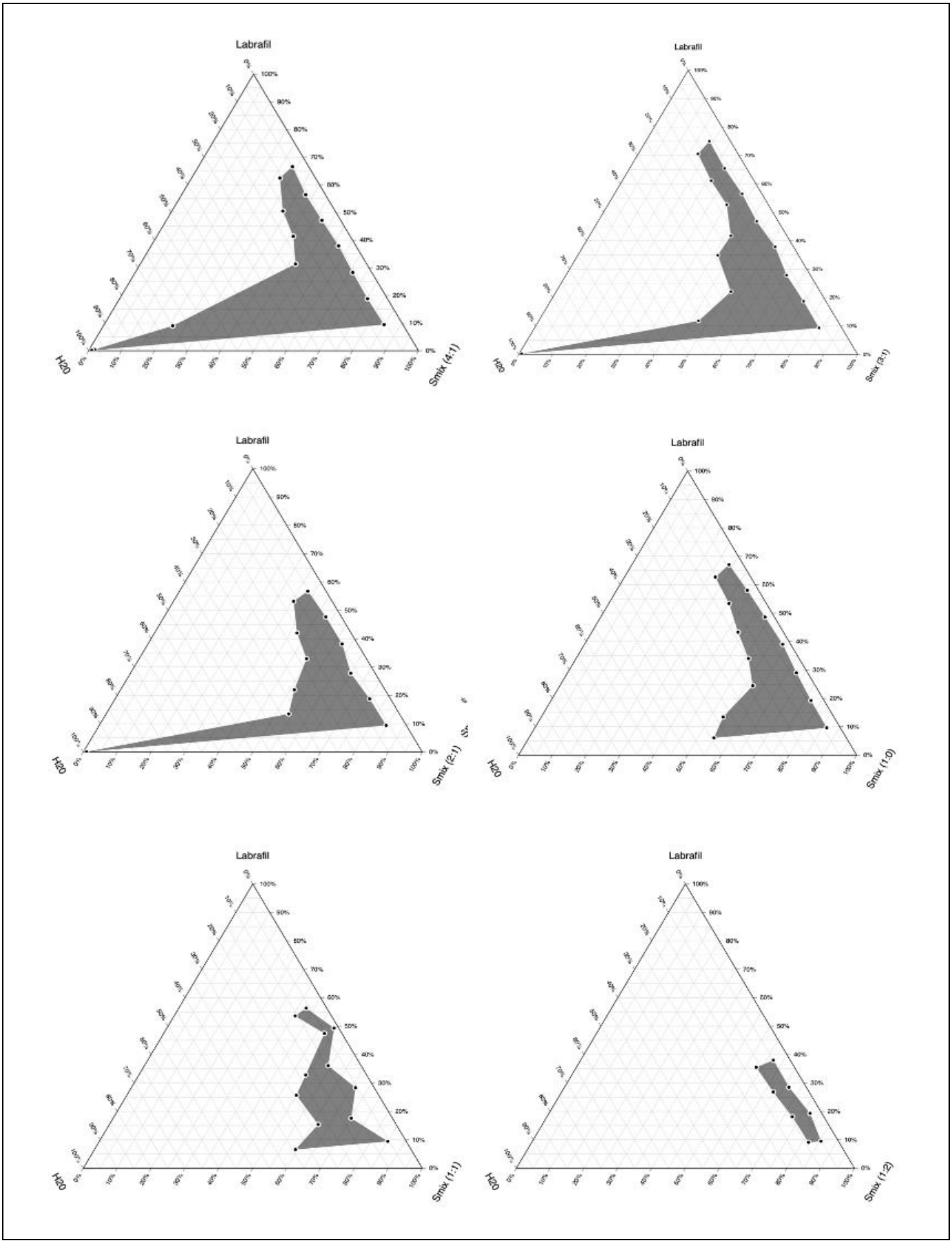

Figure 5. Pseudo-ternary phase diagrams of the oil-surfactant-water system at 1:0, 1:2, 1:1, 2:1, 3:1, 4:1 at weight ratios of Tween 80 to Transcutol HP. The dark region represents the nanoemulsion areas, while the clear region shows that the compositions did not produce nanoemulsions.

Table 4. Composition and characterization of various ADG-SNEDDS formulations (mean ± SD, n=3).

Composition (g)	O:S_{mix} = 3:7			O:S_{mix} = 4:6		
	F1	**F2**	**F3**	**F4**	**F5**	**F6**
Andrographolide	0.2	0.2	0.2	0.2	0.2	0.2
LabrafilM1944CS	5	10	15	5	10	15
S_{mix}	11.6	23.3	35.0	7.5	15.0	22.5
H_2O	100	100	100	100	100	100
Droplet size (nm)	92.6 ± 1.3	145.5 ± 2.7	156.6 ± 3.9	215.2 ± 3.6	181.9 ± 2.0	175.4 ± 1.8
PDI	0.544 ± 0.000	0.226 ± 0.008	0.292 ± 0.012	0.500 ± 0.038	0.370 ± 0.025	0.420 ± 0.016

unstable nanoemulsion system. Thus, F2 was chosen as the optimized formulation because of its small droplet size (145.5 ± 2.7 nm) and low PDI (0.226 ± 0.008).

3.3 Cell viability

Renal cell lines were treated with optimized formulations of micelle polymer and SNEDDS, along with AGD-loaded suspension. The control sample was medium containing RPMI-1640 only.

In the blank samples, polymer concentration was prepared in the range of 0.1 – 20.0 mg/mL to cover the polymer amounts corresponding to those used in ADG-loaded formulations, while the blank SNEDDS samples were prepared with the same ratios of oil, surfactant, and co-surfactant as the corresponding ADG-loaded formulations. The ADG-loaded samples C1–C6 were prepared with ADG concentrations of 1, 5, 10, 50, 100, and 200 μM. After 72 hours of incubation, the results in Figure 6 showed that cells treated with both blank samples showed no differences in cell density compared to the control sample (>96%), indicating that RAFT polymer and excipients in SNEDDS did not affect the cell viability.

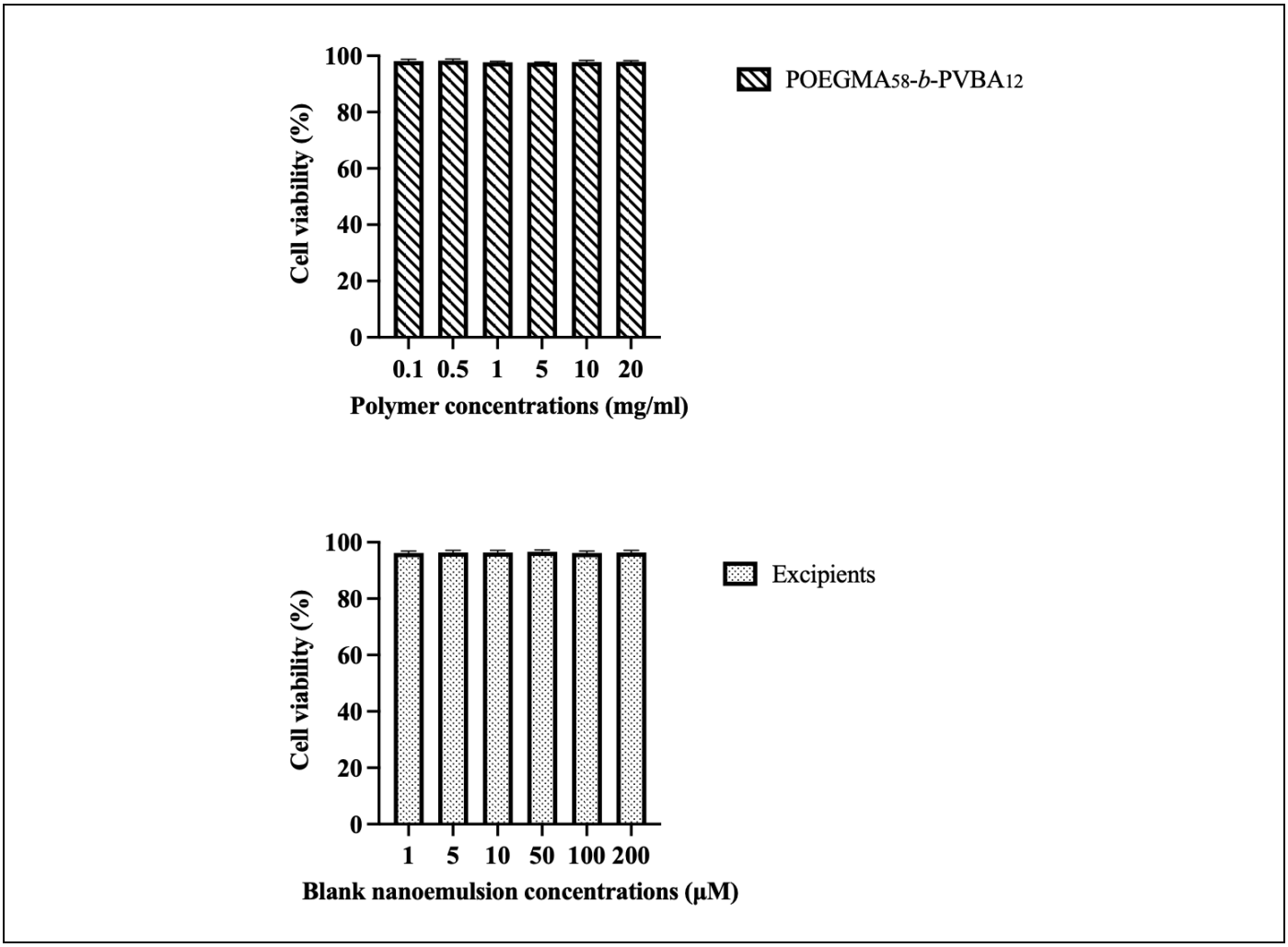

Figure 6. Cell viability of blank samples of micelle polymer and SNEDDS (mean ± SD, n=6).

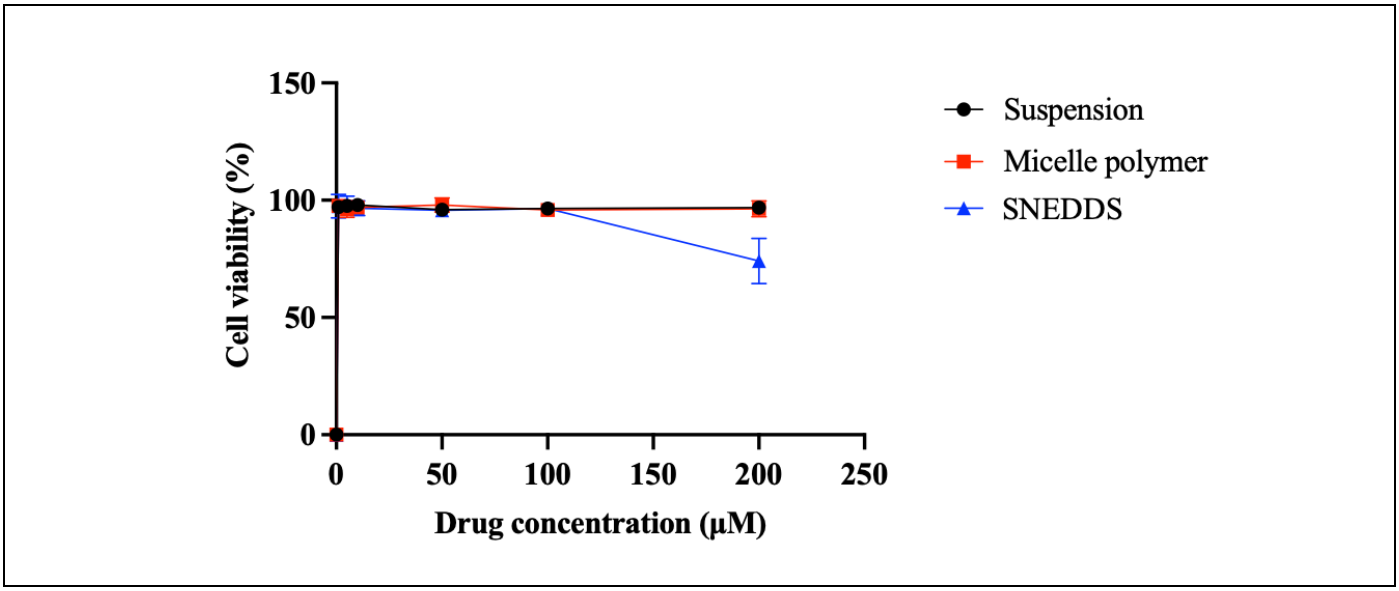

Figure 7. Cell viability assays of ADG micelle polymer, SNEDDS, and suspension (mean ± SD, n=6).

The results of cell viability assays of the three samples are shown in Figure 7. Cells treated with ADG polymeric micelle and suspension showed no difference in cell density and remained above 95%. In contrast, treatment with SNEDDS formulation C6 at 200 µM ADG, which contained the same amount of SNEDDS excipients as blank sample C6, significantly reduced cell viability to 74.2%. This may be due to surfactants and cosurfactants in the SNEDDS formulations, as these components could reduce the interfacial tension and increase the permeability of the drug substance. In addition, small droplet size in SNEDDS provides a larger surface area, and enables better adherence and absorption to the membrane during drug transport[30], hence increasing intracellular concentrations and toxicity to cells compared to other samples.

From the results, we were unable to determine the 50% inhibitory dose (IC_{50}) of ADG for the Renca cell line at the concentration 1-200 µM. Compared with other drug substances, results showed that axitinib reduced 60% of cells at the concentration of 100nM[31], and sorafenib at only 5 µM exhibited significant cytotoxic effects on Renca cells[32]. Other research suggested that IC_{50} values of ADG were 31.93 ± 0.04 µM for MCF-7 cells – a breast cancer cell line, after 72 hours[33], and 15 µM for colon cancer cell lines[34], suggesting a weak cytotoxic effect against kidney cancer due to a high IC_{50} value (> 200 µM). However, these results support the rationale for using nanocarrier-based delivery systems, especially SNEDDS, to potentiate the intracellular delivery of poorly soluble compounds like ADG. Further optimization of the formulation and targeted delivery strategies could help improve the anticancer efficacy of ADG in renal cancer therapy.

4. DISCUSSION

The present study focused on the development of SNEDDS and polymeric micelles loaded with ADG and the evaluation of these systems on the Renca cell line. Interestingly, only the SNEDDS formulation exhibited significant cytotoxicity, while the polymeric micelles showed no significant effect under the same experimental conditions.

Previous studies have demonstrated that the polymeric micelle system can be effective against renal cancer models. For example, NK012 polymeric micelles loaded with camptothecin derivatives showed antitumor activity against Renca tumors[35], while a Vitamin E–TPGS–based nanomicelle formulation loaded with CARP-1 has enhanced the drug solubility and demonstrated potent growth inhibition in Everolimus-resistant RCC cells[36]. In contrast, the lack of cytotoxic activity observed with POEGMA-*b*-PVBA micelles in our study may be attributed to several factors. Firstly, the strong hydrophobic interactions between the PVBA core and the drug may lead to slow drug release, resulting in low drug concentrations during the assay period. Secondly, the dense hydrophilic POEGMA corona, which could reduce opsonization and prolong systemic circulation *in vivo*, may substantially reduce membrane interactions *in vitro*, leading to lower rates of cellular uptake and hence limited intracellular drug exposure. For example, previous studies on micelles with varying PEG chain lengths demonstrated that formulations with larger PEG coronas exhibited reduced cellular internalization compared to those with shorter PEG chains, due to decreased surface charge and limited electrostatic interactions with the cell membrane[37]. A similar mechanism may also contribute to the limited

uptake of POEGMA-based micelles in our study. However, an important point to emphasize is that although our results indicate a clear advantage of SNEDDS over polymeric micelles *in vitro* conditions, this does not necessarily indicate that micelles are ineffective against renal cancer cells. The lack of activity observed in our study may reflect the incompatibility between the POEGMA-*b*-PVBA and Andrographolide, rather than a limitation of the micelle systems.

On the other hand, the SNEDDS system generated nanoemulsified droplets when diluted, providing rapid drug release and enhanced permeability from its surfactant components. Such characteristics are consistent with previous studies of SNEDDS improving cellular uptake and cytotoxicity of poorly soluble agents. Although no studies have yet investigated SNEDDS specifically in renal cancer cell lines, similar outcomes confirming the impact of this delivery system have been reported in other cancer models. For instance, a study showed that curcumin-phospholipid SNEDDS enhanced cytotoxic activity in metastatic breast carcinoma cells and reduced tumour growth[38]. Many studies are consistent with our findings, where the formulation's characteristics (nano-sized droplets and permeability enhancement due to lipids and surfactants) improved intracellular delivery to the cells. In addition, the presence of surfactants in SNEDDS not only stabilizes the formulation but also directly contributes to improved permeability and P-gp efflux inhibition, both of which are crucial factors in overcoming drug resistance in RCC. For Andrographolide, which exhibits poor solubility and is susceptible to efflux transport, these advantages are particularly meaningful. Moreover, while many prior renal applications of SNEDDS focused on mitigating nephrotoxicity[39], our study concentrates on anticancer therapy, aiming to enhance cytotoxicity. This highlights an important point, which is that SNEDDS can be applied not only to enhance drug solubility but also to direct pharmacological activity toward renal tissues.

To our knowledge, few studies have evaluated Andrographolide's effects on renal cancer. A study demonstrated that Andrographolide has been shown to sensitize renal cancer cells to TRAIL signaling by upregulating death receptor 4 (DR4)[40]**,** highlighting its potential in renal cancer therapy. However, ADG is limited by its low aqueous solubility and susceptibility to efflux transport, all of which restrict its intracellular accumulation. Although ADG-SNEDDS formulations have been developed and characterized in many previous studies, we did not find studies of ADG-loaded SNEDDS evaluated specifically on renal cancer models. Given the fact that renal cell carcinoma exhibits strong drug resistance driven by multiple mechanisms, this type of cancer is particularly challenging to treat, as many factors could reduce intracellular drug concentration and therapeutic efficacy. Therefore, our study provides novel data on the potential of SNEDDS to enhance ADG intracellular delivery and cytotoxicity in renal cancer cells.

5. CONCLUSIONS

In this study, ADG-loaded micelle polymer and SNEDDS were formulated after evaluating various factors to find the optimum formulations. ADG-loaded micelle polymer was prepared successfully using the RAFT polymerization technique. POEGMA-*b*-PVBA polymer was synthesized in advance and conjugated with ADG, exhibiting a nanoparticle size and a narrow size distribution. ADG was also prepared as SNEDDS with Labrafil 1944 CS, Tween 80, and Transcutol HP, with a particle size of 145.5 ± 2.7 nm. In addition, we compared the anticancer activity of these two systems on the Renca cell line with ADG suspension. The cell viability only reduced significantly to 74.2% after incorporation with ADG-loaded SNEDDS at 200 μM, whereas ADG polymeric micelle and suspension showed no influence. The results indicated that the SNEDDS significantly improved the cytotoxic activity of ADG compared to polymeric micelles, suggesting better delivery efficiency and cellular uptake.

6. ACKNOWLEDGEMENTS

Author contribution

Category 1

Conception and design of study: Nguyen-Thach Tung

Acquisition of data: Ngoc-Quang Do, Nhat-Trang Nguyen, Tran-Mai-Phuong Nguyen

Analysis and/or interpretation of data: Nguyen-Thach Tung, Nhat-Trang Nguyen,

Ngoc-Quang Do, Tran-Mai-Phuong Nguyen, Cong-Khanh Cao, Thi-Thu-Hien Duong

Category 2

Drafting the manuscript: Nhat-Trang Nguyen, Tran-Mai-Phuong Nguyen

Revising the manuscript critically for important intellectual content: Nguyen-Thach Tung

Category 3

Approval of the version of the manuscript to be published: Nguyen-Thach Tung, Thi

Thu-Hien Duong, Nhat-Trang Nguyen, Ngoc-Quang Do, Tran-Mai-Phuong Nguyen,

Cong-Khanh Cao

Funding

This research is funded by the Vietnam National Foundation for Science and Technology Development (NAFOSTED) under grant number 108.05-2023.01

Conflict of interest
None to declare.

Ethics approval
None to declare.

Article info:
Received May 12, 2025
Received in revised form September 17, 2025
Accepted February 14, 2026

REFERENCES

1. Porta C, Cosmai L, Leibovich BC, Powles T, Gallieni M, Bex A. The adjuvant treatment of kidney cancer: a multidisciplinary outlook. Nat Rev Nephrol. 2019;15(7):423–33.
2. Banerjee M, Parai D, Chattopadhyay S, Mukherjee SK. Andrographolide: antibacterial activity against common bacteria of human health concern and possible mechanism of action. Folia Microbiol (Praha). 2017;62(3):237–44.
3. Li B, Jiang T, Liu H, Miao Z, Fang D, Zheng L, et al. Andrographolide protects chondrocytes from oxidative stress injury by activation of the Keap1–Nrf2–Are signaling pathway. J Cell Physiol. 2019;234(1):561–71.
4. Lim JCW, Goh FY, Sagineedu SR, Yong ACH, Sidik SM, Lajis NH, et al. A semisynthetic diterpenoid lactone inhibits NF-κB signalling to ameliorate inflammation and airway hyperresponsiveness in a mouse asthma model. Toxicol Appl Pharmacol. 2016;302:10–22.
5. Ahmed S, Kwatra M, Ranjan Panda S, Murty USN, Naidu VGM. Andrographolide suppresses NLRP3 inflammasome activation in microglia through induction of parkin-mediated mitophagy in in-vitro and in-vivo models of Parkinson disease. Brain Behav Immun. 2021;91:142–58.
6. Zhang R, Zhao J, Xu J, Jiao DX, Wang J, Gong ZQ, et al. Andrographolide suppresses proliferation of human colon cancer SW620 cells through the TLR4/NF-κB/MMP-9 signaling pathway. Oncol Lett. 2017;14(4):4305–10.
7. Luo X, Luo W, Lin C, Zhang L, Li Y. Andrographolide inhibits proliferation of human lung cancer cells and the related mechanisms. Int J Clin Exp Med. 2014;7(11):4220–5.
8. Alshora DH, Ibrahim MA, Alanazi FK. Chapter 6 - Nanotechnology from particle size reduction to enhancing aqueous solubility. In: Grumezescu AM, editor. Surface Chemistry of Nanobiomaterials [Internet]. William Andrew Publishing; 2016 [cited 2025 Feb 21]. p. 163–91. Available from:https://www.sciencedirect.com/science/article/pii/B9780323428613000066
9. Kou L, Bhutia YD, Yao Q, He Z, Sun J, Ganapathy V. Transporter-guided delivery of nanoparticles to improve drug permeation across cellular barriers and drug exposure to selective cell types. Front Pharmacol. 2018;9:27.
10. Kumar S, Dilbaghi N, Saharan R, Bhanjana G. Nanotechnology as emerging tool for enhancing solubility of poorly water-soluble drugs. BioNanoScience. 2012;2(4):227–50.
11. Porter CJH, Trevaskis NL, Charman WN. Lipids and lipid-based formulations: optimizing the oral delivery of lipophilic drugs. Nat Rev Drug Discov. 2007;6(3):231–48.
12. Krstić M, Medarević Đ, Đuriš J, Ibrić S. Self-nanoemulsifying drug delivery systems (SNEDDS) and self-microemulsifying drug delivery systems (SMEDDS) as lipid nanocarriers for improving dissolution rate and bioavailability of poorly soluble drugs. In: Lipid Nanocarriers for Drug Targeting [Internet]. Elsevier; 2018 [cited 2025 Feb 13]. p. 473–508. Available from:https://linkinghub.elsevier.com/retrieve/pii/B9780128136874000128
13. Khan AW, Kotta S, Ansari SH, Sharma RK, Ali J. Potentials and challenges in self-nanoemulsifying drug delivery systems. Expert Opin Drug Deliv. 2012;9(10):1305–17.
14. Baloch J, Sohail MF, Sarwar HS, Kiani MH, Khan GM, Jahan S, et al. Self-nanoemulsifying drug delivery system (SNEDDS) for improved oral bioavailability of chlorpromazine: *In vitro* and *in vivo* evaluation. Medicina (Mex). 2019;55(5):210.
15. Kim DH, Kim JY, Kim RM, Maharjan P, Ji YG, Jang DJ, et al. Orlistat-loaded solid SNEDDS for the enhanced solubility, dissolution, and *in vivo* performance. Int J Nanomedicine. 2018;13:7095–106.
16. Dastgerdi NK, Dastgerdi NK, Bayraktutan H, Costabile G, Atyabi F, Dinarvand R, et al. Enhancing siRNA cancer therapy: Multifaceted strategies with lipid and polymer-based carrier systems. Int J Pharm. 2024;663:124545.
17. Ghosh B, Biswas S. Polymeric micelles in cancer therapy: State of the art. J Controlled Release. 2021;332:127–47.
18. Barner-Kowollik C. Handbook of RAFT polymerization. John Wiley & Sons; 2008. 560 p.
19. Moad G. RAFT Polymerization – Then and now. In: Matyjaszewski K, Sumerlin BS, Tsarevsky NV, Chiefari J, editors. ACS symposium series [Internet]. Washington, DC: American Chemical Society; 2015 [cited 2025 Feb 21]. p. 211–46. Available from: https://pubs.acs.org/doi/abs/10.1021/bk-2015-1187.ch012
20. Mitsukami Y, Donovan MS, Lowe AB, McCormick CL. Water-soluble polymers. 81. Direct synthesis of hydrophilic styrenic-based homopolymers and block copolymers in aqueous solution via RAFT. Macromolecules. 2001;34(7):2248–56.
21. Zhao J, Yang G, Liu H, Wang D, Song X, Chen Y. Determination of andrographolide, deoxyandrographolide and neoandrographolide in the Chinese herb *Andrographis paniculata* by micellar electrokinetic capillary chromatography. Phytochem Anal. 2002;13(4):222–7.
22. Kim S, Shi Y, Kim JY, Park K, Cheng JX. Overcoming the barriers in micellar drug delivery: loading efficiency, *in vivo* stability, and micelle–cell interaction. Expert Opin Drug Deliv. 2010;7(1):49–62.
23. Lu Y, Yue Z, Xie J, Wang W, Zhu H, Zhang E, et al. Micelles with ultralow critical micelle concentration as carriers for drug delivery. Nat Biomed Eng. 2018;2(5):318–25.
24. Yao M, Li Z, Julian McClements D, Tang Z, Xiao H. Design of nanoemulsion-based delivery systems to enhance intestinal lymphatic transport of lipophilic food bioactives: Influence of oil type. Food Chem. 2020;317:126229.
25. Gurjar R, Chan CYS, Curley P, Sharp J, Chiong J, Rannard S, et al. Inhibitory effects of commonly used excipients on p-glycoprotein *in vitro*. Mol Pharm. 2018;15(11):4835–42.
26. Soliman KA, Ibrahim HK, Ghorab MM. Formulation of risperidone as self-nanoemulsifying drug delivery system in form of effervescent tablets. J Dispers Sci Technol. 2012;33(8):1127–33.
27. Zeng L, Liu Y, Pan J, Liu X. Formulation and evaluation of norcanthridin nanoemulsions against the Plutella xylostella (Lepidotera: Plutellidae). BMC Biotechnol. 2019;19(1):16.
28. Agubata CO, Nzekwe IT, Obitte NC, Ugwu CE, Attama AA, Onunkwo GC. Effect of oil, surfactant and co-surfactant concentrations on the phase behavior, physicochemical properties and drug release from self-emulsifying drug delivery systems. [cited 2025 May 9]; Available from:https://austinpublishinggroup.com/drug-development/fulltext/drug-v1-id1005.php
29. Alshora DH, Ibrahim MA, Alanazi FK. Nanotechnology from particle size reduction to enhancing aqueous solubility. In: surface chemistry of nanobiomaterials [Internet]. Elsevier; 2016 [cited 2025 Feb 21]. p. 163–91. Available from: https://linkinghub.elsevier.com/retrieve/pii/B9780323428613000066

30. Monteiro LM, Lione VF, do Carmo FA, do Amaral LH, da Silva JH, Nasciutti LE, et al. Development and characterization of a new oral dapsone nanoemulsion system: permeability and in silico bioavailability studies. Int J Nanomedicine. 2012;7:5175–82.
31. Watanabe H, Matsushita Y, Tamura K, Motoyama D, Sugiyama T, Otsuka A, et al. Assessments of therapeutic effects according to timings for combined therapy with axitinib and immune check point inhibitor in a mouse renal cell carcinoma model. Sci Rep. 2023;13(1):11361.
32. Harada K, Miyake H, Kusuda Y, Fujisawa M. Characterization of mechanism involved in acquired resistance to sorafenib in a mouse renal cell cancer Renca model. Clin Transl Oncol. 2014;16(9):801–6.
33. Tohkayomatee R, Reabroi S, Tungmunnithum D, Parichatikanond W, Pinthong D. Andrographolide exhibits anticancer activity against breast cancer cells (MCF-7 and MDA-MB-231 Cells) through suppressing cell proliferation and inducing cell apoptosis via inactivation of ER-α receptor and PI3K/AKT/mTOR signaling. Molecules. 2022 ;27(11):3544.
34. Lim JCW, Jeyaraj EJ, Sagineedu SR, Wong WSF, Stanslas J. SRS06, a new semisynthetic andrographolide derivative with improved anticancer potency and selectivity, inhibits nuclear factor-κB nuclear binding in the A549 non-small cell lung cancer cell line. Pharmacology. 2015;95(1–2):70–7.
35. Sumitomo M, Koizumi F, Asano T, Horiguchi A, Ito K, Asano T, et al. Novel SN-38–incorporated polymeric micelle, NK012, strongly suppresses renal cancer progression. Cancer Res. 2008;68(6):1631–5.
36. Cheriyan VT, Alsaab HO, Sekhar S, Stieber C, Kesharwani P, Sau S, et al. A CARP-1 functional mimetic loaded vitamin E-TPGS micellar nano-formulation for inhibition of renal cell carcinoma. Oncotarget. 2017;8(62):104928–45.
37. Miteva M, Kirkbride KC, Kilchrist KV, Werfel TA, Li H, Nelson CE, et al. Tuning PEGylation of mixed micelles to overcome intracellular and systemic siRNA delivery barriers. Biomaterials. 2015;38:97–107.
38. Shukla M, Jaiswal S, Sharma A, Srivastava PK, Arya A, Dwivedi AK, et al. A combination of complexation and self-nanoemulsifying drug delivery system for enhancing oral bioavailability and anticancer efficacy of curcumin. Drug Dev Ind Pharm. 2017;43(5):847–61.
39. Jain S, Kambam S, Thanki K, Jain AK. Cyclosporine A loaded self-nanoemulsifying drug delivery system (SNEDDS): implication of a functional excipient based co-encapsulation strategy on oral bioavailability and nephrotoxicity. RSC Adv. 2015;5(61):49633–42.
40. Bi R, Deng Y, Tang C, Xuan L, Xu B, Du Y, et al. Andrographolide sensitizes human renal carcinoma cells to TRAIL-induced apoptosis through upregulation of death receptor 4. Oncol Rep [Internet]. 2020 Aug 18 [cited 2025 Oct 1]; Available from: http://www.spandidos-publications.com/10.3892/or.2020.7737